

Magnetic ground state of $LBaCo_2O_{5.5/5.44}$ cobalt oxides

D. D. Khalyavin

Institute of Solid State and Semiconductors Physics, National Academy of Sciences, P. Brovka str. 17, 220072 Minsk, Belarus

(Received 14 July 2004; revised manuscript received 20 July 2005; published 6 October 2005)

The magnetic properties of $LBaCo_2O_{5+\gamma}$ cobalt oxides with different types of oxygen ions ordering within $[LO_\gamma]$ layers are discussed. Symmetry arguments are used to analyze the models of the magnetic ground state proposed for these compounds. By postulating the ordering between octahedrally coordinated cobalt ions in different spin states the magnetic structures explaining a variety of observed experimental data and consisting with the symmetry analysis are presented.

DOI: [10.1103/PhysRevB.72.134408](https://doi.org/10.1103/PhysRevB.72.134408)

PACS number(s): 75.25.+z, 75.50.Gg, 75.30.Cr, 61.66.Fn

The discovery of the giant magnetoresistance and metal-insulator transition in $LBaCo_2O_{5+\gamma}$ (L =lanthanide or Y) cobalt oxides stimulated their intensive investigations.¹⁻⁴ The crystal structure of these compounds is closely related to the $YBaFeCuO_5$ -type structure and represents a sequence of $[CoO_2]$ - $[BaO]$ - $[CoO_2]$ - $[LO_\gamma]$ layers stacked along the $[001]$ axis. When the concentration of oxygen vacancies in the $[LO_\gamma]$ layers is maximum ($\gamma=0$) all cobalt cations are located within square pyramids with fivefold coordination. As γ increases, extra oxygen ions occupy vacant sites in $[LO_\gamma]$ layers, thus providing an octahedral environment for a part of the Co ions. Two types of superstructure, $a_p \times 2a_p \times 2a_p$ (122) at $\gamma=0.50$ [Fig. 1(a)] and $3a_p \times 3a_p \times 2a_p$ (332) at $\gamma=0.44$ [Fig. 1(b)], may be formed due to ordering of the extra oxygen; this corresponds to orthorhombic ($Pmmm$) and tetragonal ($P4/mmm$) symmetry of the crystal structure, respectively.⁴⁻⁶

The magnetic behavior of $LBaCo_2O_{5+\gamma}$ depends strongly on oxygen content and to a much lesser degree on L type.⁴ At $\gamma=0$ the compounds are antiferromagnets below 340 K.^{7,8} The ions of both divalent and trivalent cobalt adopt the high-spin state and form G -type spin-ordered configurations. In the case of $\gamma=0.50$ and $\gamma=0.44$ the magnetic behavior is more complex. At low temperatures, below $T_i \sim 240$ K, the state is antiferromagnetic. Above T_i a spontaneous magneti-

zation appears. This phase transition is accompanied by a jump of resistivity. Below T_i , the state with spontaneous magnetization can be induced by external magnetic fields, which, in combination with the strong coupling between magnetic and electrical properties, gives the giant magnetoresistance phenomenon. Around $T_C \sim 290$ K the spontaneous magnetization disappears. A further enhancement of temperature results in one more magnetic phase transition around $T_N \sim 340$ K, at which an increase of the effective paramagnetic moment occurs. In the temperature range $T_C < T < T_N$, the inverse magnetic susceptibility obeys the Curie-Weiss law with a positive paramagnetic Curie temperature $\theta \sim 280$ K. Above T_N , the θ becomes negative. For the compounds with the 122 type of the crystal structure, the phase transition at T_N was reported to be accompanied by a transformation to a metallic conductivity, whereas for the compounds with the 332 structural type, the anomaly of the magnetic susceptibility does not lead to a clear anomaly in the electrical properties.²⁻⁵ Measurements of the heat capacity⁹ revealed a low-entropy change at T_C and much higher one at T_N , which was interpreted as the establishment of a short-range magnetic ordering at this temperature.

The magnetic ground state of $LBaCo_2O_{5.5/5.44}$ cobalt oxides and the nature of the phase transformations are widely discussed in the literature. In spite of the difference in the crystal structures, the very similar magnetic properties of the compounds with $\gamma=0.50$ and $\gamma=0.44$ allow us to assume that the magnetic ground states of these structural types are very similar too. Several models have been proposed but none of them can explain all the observed experimental data. The general problem is the nature of the spontaneous magnetization within the temperature range $T_i < T < T_C$ and the strong coupling between magnetic and electrical properties. One of the first ideas was the model involving an antiferromagnetic ordering with a small ferromagnetic component due to the Dzyaloshinskii-Moriya-type interactions.^{5,10,11} The value of the spontaneous magnetization (σ_s) obtained from magnetic measurements of polycrystalline samples $\sim 0.15\mu_B$ per Co ion^{5,10} did not contradict this assumption. The powder neutron diffraction spectra of $NdBaCo_2O_{5.47}$ were also refined assuming the G -type antiferromagnetic ordering within this temperature range.¹² However, a recent success in single-crystal growth of these cobaltites^{13,14} clarified several important moments. In particular, a strong magnetic anisotropy

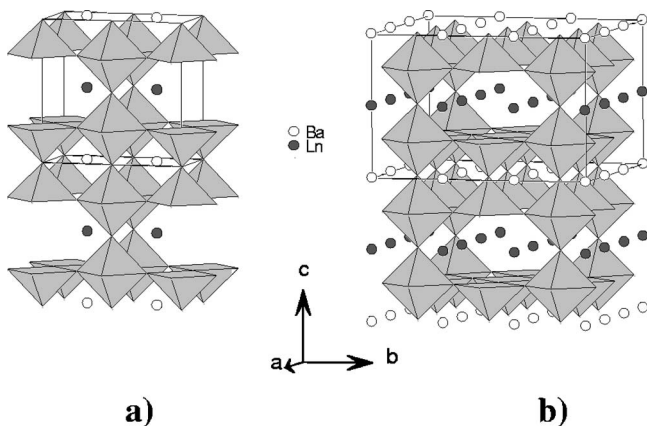


FIG. 1. Polyhedral representation of the crystal structure of $LBaCo_2O_{5.5}$ with $a_p \times 2a_p \times 2a_p$ (122) type of superstructure (a) and $LBaCo_2O_{5.44}$ with $3a_p \times 3a_p \times 2a_p$ (332) type of superstructure (b).

TABLE I. Basis functions (S^k) of irreducible representations of the $Pmma$ space group, entering the magnetic representation on $2e(1/4 0 z; z \sim \pm 1/4)$ and $2f(1/4 1/2 z; z \sim \pm 1/4)$ positions, with $k=0$.

irrep	Γ_2^+	Γ_3^+	Γ_4^+	Γ_1^-	Γ_3^-	Γ_4^-
i^a	1	2	1	2	1	2
$2e$	$1/4 0 z$	$3/4 0 -z$	$1/4 0 z$	$3/4 0 -z$	$1/4 0 z$	$3/4 0 -z$
$2f$	$1/4 1/2 z$	$3/4 -1/2 -z$	$1/4 1/2 z$	$3/4 -1/2 -z$	$1/4 1/2 z$	$3/4 -1/2 -z$
S_x^k	0	1	0	0	0	$\bar{1}$
S_y^k	0	0	1	0	1	0
S_z^k	1	0	0	1	0	0

^a i numerates cobalt ions in the $2e/2f$ positions; the coordinates of the symmetry linked ions are presented too.

was revealed, which is the reason for the small value of the spontaneous magnetization obtained on polycrystalline samples. The real value of σ_s , coming from the magnetic measurements on the single crystals, is $\sim 1\mu_B$ per Co ion at $T=0$ K. This fact argues for the model involving a 1:1 mixture of the cobalt ions in the low-spin state and ferromagnetically ordered cobalt ions in the intermediate-spin state. Besides the exact value of the spontaneous magnetization, this model gives a physically reasonable explanation of the metamagnetic behavior and the magnetotransport phenomenon as well as agrees well with the positive value of θ .¹³⁻¹⁵ But this model contradicts the neutron diffraction data.¹² The aim of the present work is to analyze the existent experimental data to propose a model which is entirely consistent with them.

According to Fauth *et al.*¹² the magnetic structure of $NdBaCo_2O_{5.47}$ above T_i is characterized by the propagation vector $k=[1/2 0 0]$ applied to the $a_p \times 2a_p \times 2a_p$ crystal lattice. The symmetry condition for a nonzero spontaneous magnetic moment is $k=0$. To satisfy this condition the crystal structure must be doubled along the a direction ($2a_p \times 2a_p \times 2a_p$ unit cell). This means that there are four nonequivalent cobalt positions in $LBaCo_2O_{5.5}$ oxides. In other words, the crystal structure involves nonequivalent cobalt ions with the same coordination. A similar conclusion was arrived at by Itoh *et al.*¹⁶ and Kubo *et al.*¹⁷ based on NMR measurements of ^{59}Co nuclei in $YBaCo_2O_{5.5}$ and $EuBaCo_2O_{5.5}$, respectively.

Very recently Chernenkov *et al.*¹⁸ have found weak superstructure reflections doubling the a axis in $GdBaCo_2O_{5.5}$ single crystals. The systematic extinction of these reflections points to the $Pmma$ space group. Two possible reasons for the a axis doubling have been proposed: orbital ordering and/or ordering of the cobalt ions in different spin states. The formation of the different superstructures at spin-state transitions has been theoretically justified by Khomskii and Löw.¹⁹ Earlier, Fauth *et al.*¹² introduced the spin-state-ordered phase to interpret the low-temperature neutron diffraction data for $NdBaCo_2O_{5.47}$. The basic assumption of the given work is also the postulation of a long-range ordering between cobalt ions with different $3d^6$ electronic configurations.

It has been shown that the ground state of Co^{3+} ions in the CoO_5 pyramidal coordination is the state with the high-spin electronic configuration. This conclusion comes from neutron diffraction data for the $LBaCo_2O_5$ series^{7,8,20} and both neutron diffraction²¹ and soft x-ray absorption spectroscopy²² for Sr_2Co_3Cl , as well as being confirmed by LDA+ U calculations.^{22,23} Therefore, following these results we should conclude that fivefold-coordinated cobalt ions in $LBaCo_2O_{5.5/5.44}$ perovskites adopt the high-spin state, whereas the superstructure develops in the position containing only sixfold-coordinated cobalt.

In the beginning we will consider the compounds with the 122 crystal structure and then we will show that the obtained results can be easily extrapolated on the 332 structural type. The cobalt ions occupy four independent positions in the $Pmma$ space group with $2a_p \times 2a_p \times 2a_p$ unit cell: Co1- $2e(1/4 0 -z)$, Co2- $2e(1/4 0 z)$, Co3- $2f(1/4 1/2 -z)$, and Co4- $2f(1/4 1/2 z)$; in all cases, $z \sim 1/4$, which corresponds to the chessboardlike ordering between cobalt ions in different spin states. These positions are characterized by the

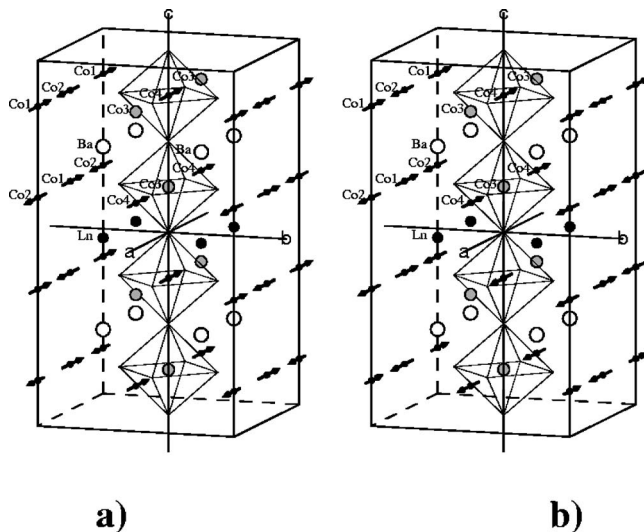


FIG. 2. Schematic representation of the magnetic structure above T_i (a) and below T_i (b) for $LBaCo_2O_{5.5}$ compounds with the 122 type of crystal structure. Cobalt ions in the low-spin state (Co3) are denoted by gray circles

same transformational properties. One should note that the directions of the basis vectors, for both the $Pmmm$ (spin-stated disordered phase) and the $Pmma$ (spin-state ordered phase) space groups, coincide. Therefore, when we use the designations a , b , and c for the crystallographic axes, we will not refer to a certain space group ($Pmmm$ or $Pmma$). Sup-

pose Co1, Co2 and Co3, Co4 are the square pyramidal and octahedral positions, respectively. The formation of the superstructure, in the planes containing octahedral-coordinated cobalt (ac planes), means that the magnetic moments on the Co3 and Co4 positions can be different, whereas on the Co1 and Co2 they are equal. Since the magnetic state with spontaneous magnetization is of the main interest, we will start our consideration from this magnetic phase.

In the case of the $Pmma$ space group with $2a_p \times 2a_p \times 2a_p$ unit cell, the magnetic structure of $LBaCo_2O_{5.5}$ oxides above T_i is described by the $k=0$; i.e., the obligatory condition for a nonzero spontaneous magnetic moment is satisfied. From the eight one-dimensional irreducible representations (irreps) of $Pmma$ at $k=0$ only six enter the magnetic representation $D_m^{k=0}$ on the $2e$ and $2f$ positions:

$$D_m^{k=0}(2e) = D_m^{k=0}(2f) = \Gamma_2^+ + \Gamma_3^+ + \Gamma_4^+ + \Gamma_1^- + \Gamma_3^- + \Gamma_4^-. \quad (1)$$

Each irrep (we use the Miller-Love notations²⁴) enters only once, which means that there is only a set of linearly independent basis functions. The calculated basis functions (S^k) for these irreps are presented in Table I. The result shows that the weak ferromagnetism is forbidden by the symmetry at any antiferromagnetic configuration, which can be constructed using the basis functions from Table I. This conclusion comes from the requirement that the ferromagnetic component has to belong to the same irreducible representation of the symmetry group as the main antiferromagnetic vector. Further, from the obtained result the symmetry objec-

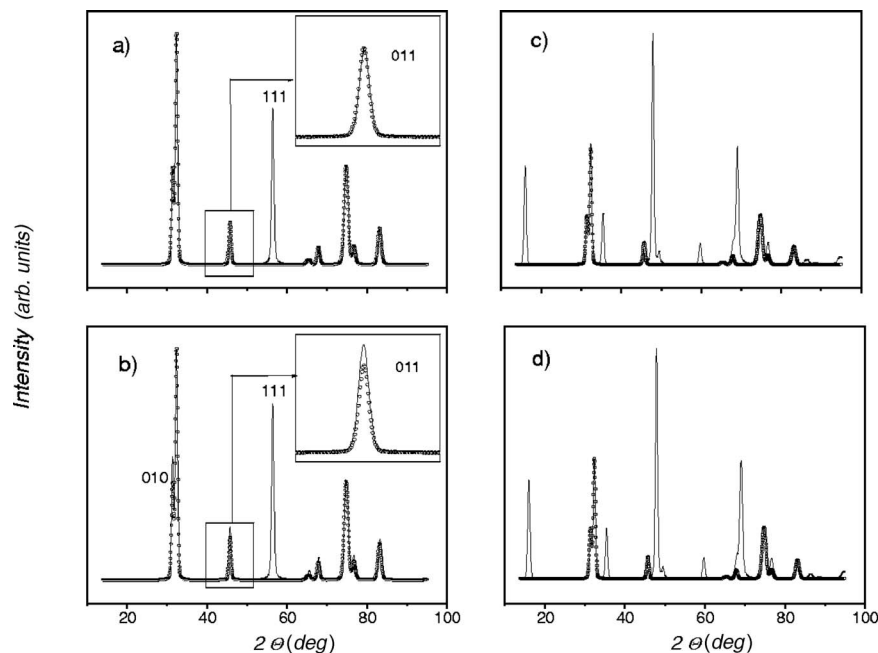


FIG. 3. Simulated neutron ($\lambda=4.2 \text{ \AA}$) diffraction spectra (solid line), involving both nuclear and magnetic scatterings, for $LBaCo_2O_{5.5}$ with different configurations of the magnetic moments of cobalt ions: (a) G -type, (b) shown in Fig. 2(a), (c) shown in Fig. 2(b), and (d) taken from Ref. 12 for the spin-state-ordered phase. In all the cases a purely paramagnetic spectrum (open circles) is presented too. Insets in the (a) and (b) panels show 011 reflection to demonstrate the presence of the magnetic contribution in the case of the spin configuration shown in Fig. 2(a). The calculation of the nuclear scattering was performed in the $Pmmm$ space group using the structural data from Ref. 26. [It was neglected that the real symmetry is $Pmma$, because the reflections arising from the electronic ordering (spin-state ordering) are extremely weak and can be apparently observed only in single crystals.] The simulation was performed with the aid of the FULLPROF program (Ref. 29).

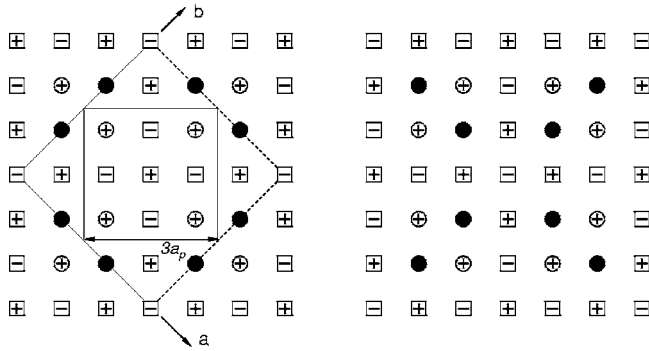


FIG. 4. Schematic representation of the two neighbor (001) planes, containing cobalt ions in different coordination, for compounds with the 332 type of crystal structure. Cobalt ions in the octahedral and pyramidal coordinations are presented by circles (dark, in the low-spin state; open, in the high-spin state) and squares, respectively. The positive (+) and negative (-) directions of the magnetic moments on the paramagnetic ions are shown too.

tions against the high-temperature magnetic structure for $\text{TbBaCo}_2\text{O}_{5.5}$ proposed by Soda *et al.*²⁵ follow, because this model involves the basis functions of more than a single irrep. Sometimes, in the case of a negligible small magnetic anisotropy in comparison with the exchange interactions, a magnetic structure can be formed by the basis functions of the different irreps of the given space group. However, these irreps have to belong to a single exchange multiplet corresponding to a single irreducible representation of the symmetry group of the exchange Hamiltonian. In the case of $\text{LBaCo}_2\text{O}_{5.5}$, (i) anisotropic interactions are very strong,^{13,14} which should lead to an effective splitting of the exchange multiplets, and (ii) by considering the degenerated states, with respect to the exchange energy, it is easy to show that this argument cannot be applied for the magnetic structure proposed in Ref. 25.

Let us construct the magnetic structure for $\text{LBaCo}_2\text{O}_{5.5}$ using the basis functions from Table I. The model should satisfy the following requirements: (i) the basis functions for the cobalt positions should belong to a single irrep, (ii) the value of the spontaneous magnetization should equal $1\mu_B$ per Co ion and the magnetic moment should be directed along the a axis,¹³ and (iii) the sign of the exchange interactions between nearest neighbors should satisfy the Goodenough-Kanamory rules. These requirements unambiguously determine the model presented in Fig. 2(a). For the octahedral coordination, the magnetic moments on the Co3 and Co4 positions are 0 and $4\mu_B$, respectively, which gives $\sigma_s = 1\mu_B$ per Co ion. The obtained magnetic structure can be presented as a consequent alternation of the ferromagnetic and antiferromagnetic (ac) planes formed by sixfold- (Co4) and fivefold- (Co1 and Co2) coordinated cobalt ions, respectively.

A calculation of the magnetic intensity starting from the obtained model gives a qualitatively good agreement with the neutron diffraction data,¹² where the G -type antiferromagnetic ordering was assumed. For the G -type spin-ordered configuration the main magnetic intensity is concentrated in the 111 (for $2a_p \times 2a_p \times 2a_p$ unit cell) reflection [Fig. 3(a)]. In the case of the model presented in Fig. 2(a), the magnetic

intensity is also mainly concentrated in this reflection, but there is also a ferromagnetic contribution to the nuclear reflections such as 010 , 011 , 002 and 012 [Fig. 3(b)]. Because of the small value of the ferromagnetic component above T_i , a careful analysis of the nuclear reflections is required for this contribution to be detected.

From the obtained model it follows that each paramagnetic cobalt ion, with octahedral coordination (Co4), is exchange coupled only with two magnetoactive (which magnetic moments $\neq 0$) (Co2) ions, whereas any cobalt ion with pyramidal coordination (Co1 or Co2) is coupled not less than with three magnetoactive ions [Fig. 2(a)]. Therefore, one should expect that the ferromagnetic (ac) planes, formed by Co4 ions, become paramagnetic at lower temperature (T_C) than the antiferromagnetic planes (double pyramidal chains), formed by fivefold-coordinated cobalt (T_N). In the temperature range $T_C < T < T_N$ the magnetic susceptibility is mainly caused by the paramagnetic contribution of the octahedral (ac) planes. In addition, the antiferromagnetic exchange interactions, between sixfold-coordinated Co4 ions and fivefold-coordinated Co2 ions, are equivalent to an effective positive exchange between Co4 ions within the octahedral (ac) planes. This gives a positive value of θ . A disordering of the pyramidal (ac) planes (chains) at T_N has to be accompanied by an increase of the effective paramagnetic moment and the change of the θ sign. Thus, the high-temperature anomaly of the magnetic susceptibility can be explained without involving a spin-state transition as well as this model explains the results of the heat capacity measurements.⁹

The spin-state transition is actively involved to interpret the anomaly of the magnetic susceptibility and the metal-insulator transition in compounds with the 122 type of crystal structure.^{26,27} At the same time, in compounds with the 332 type of lattice, the analogous anomaly of the susceptibility does not affect the electrical properties.^{4,5} In addition, the recent resonant photoemission data on Gd- and Dy-based single crystals did not confirm that the phase transition at T_N is associated with a sudden low-spin \rightarrow high-spin switch of cobalt ions in the octahedral sites.²⁸

Now, let us consider the magnetic ground state below T_i . According to neutron diffraction data¹² the magnetic structure, below this temperature, is characterized by the propagation vector $k = [0 \ 0 \ 1/2]$. In this case, the magnetic representation on the $2e$ and $2f$ positions consists of the six one-dimensional irreps too:

$$D_m^{k=001/2}(2e) = D_m^{k=001/2}(2f) = Z_2^+ + Z_3^+ + Z_4^+ + Z_1^- + Z_3^- + Z_4^- \quad (2)$$

The matrices of the Z_n^\pm irreps are identical to the corresponding matrices of the Γ_n^\pm irreps. Therefore, we can use the basis functions from Table I. However, in the case of $k = [0 \ 0 \ 1/2]$ a magnetic unit cell is doubled along the c axis. This means that the nuclear translation along this axis becomes antitranslational. The most natural magnetic structure, coming from the high-temperature one, is the model constructed on the basis functions of the Z_3^+ irrep and shown in Fig. 2(b). A comparison of the magnetic intensities, calculated starting from this model [Fig. 3(c)] and the model pro-

TABLE II. Basis functions of irreducible representations of the $P4mm$ space group, entering the magnetic representations on $1a/1b$, $4d$, and $4e/4f$ positions, with $k=0$.

Wyckoff position	$1a(00z)$ $1b(1/2\ 1/2\ z)4d(x\ x\ z)$				$4e(x\ 0\ z) \rightarrow x \sim 1/3\ z \sim -1/4; x \sim 1/3\ z \sim 1/4$ $4f(x\ 1/2\ z) \rightarrow x \sim 1/6\ z \sim -1/4; x \sim 1/6\ z \sim 1/4$				
	$z \sim -1/4; z \sim 1/4$	$x \sim 1/6\ z \sim -1/4; x \sim 1/6\ z \sim 1/4$	$x \sim 1/3\ z \sim -1/4; x \sim 1/3\ z \sim 1/4$						
i^a	1 00z 1/2 1/2 z	1 x x z	2 -x -x z	3 -x x z	4 x -x z	1 x 0 z x 1/2 z	2 -x 0 z -x -1/2 z	3 0 x z -1/2 x z	4 0 -x z 1/2 -x z
Irrep.					Γ_1				
S_x^k		1	$\bar{1}$	1	$\bar{1}$	0	0	$\bar{1}$	1
S_y^k		$\bar{1}$	1	1	$\bar{1}$	1	$\bar{1}$	0	0
S_z^k		0	0	0	0	0	0	0	0
Irrep.					Γ_2				
n^b					1				
S_x^k		1	$\bar{1}$	1	$\bar{1}$	0	0	1	$\bar{1}$
S_y^k		1	$\bar{1}$	$\bar{1}$	1	1	$\bar{1}$	0	0
S_z^k		0	0	0	0	0	0	0	0
Irrep.					Γ_2				
n					2				
S_x^k		0	0	0	0				
S_y^k		0	0	0	0				
S_z^k		1	1	$\bar{1}$	$\bar{1}$				
Irrep.					Γ_3				
n					1				
S_x^k		1	$\bar{1}$	$\bar{1}$	1	1	$\bar{1}$	0	0
S_y^k		$\bar{1}$	1	$\bar{1}$	1	0	0	$\bar{1}$	1
S_z^k		0	0	0	0	0	0	0	0
Irrep.					Γ_3				
n					2				
S_x^k						0	0	0	0
S_y^k						0	0	0	0
S_z^k						1	1	$\bar{1}$	$\bar{1}$
Irrep.					Γ_4				
n					1				
S_x^k	0	0	0	0	0	0	0	0	0
S_y^k	0	0	0	0	0	0	0	0	0
S_z^k	1	1	1	1	1	1	1	1	1
n					2				
S_x^k		1	$\bar{1}$	$\bar{1}$	1	1	$\bar{1}$	0	0
S_y^k		1	$\bar{1}$	1	$\bar{1}$	0	0	1	$\bar{1}$
S_z^k		0	0	0	0	0	0	0	0
Irrep.					Γ_5				
n					1				
j^c	1 2	1 2	1 2	1 2	1 2	1 2	1 2	1 2	1 2
S_x^k	0 1	1 1	1 1	$\bar{1}$ 1	$\bar{1}$ 1	0 0	0 0	0 $\bar{1}$	0 $\bar{1}$
S_y^k	$\bar{1}$ 0	$\bar{1}$ $\bar{1}$	$\bar{1}$ $\bar{1}$	$\bar{1}$ 1	$\bar{1}$ 1	1 0	1 0	0 0	0 0
S_z^k	0 0	0 0	0 0	0 0	0 0	0 0	0 0	0 0	0 0
n					2				
S_x^k		1 $\bar{1}$	1 $\bar{1}$	$\bar{1}$ $\bar{1}$	$\bar{1}$ $\bar{1}$	0 1	0 1	0 0	0 0
S_y^k		1 $\bar{1}$	1 $\bar{1}$	1 1	1 1	0 0	0 0	$\bar{1}$ 0	$\bar{1}$ 0
S_z^k		0 0	0 0	0 0	0 0	0 0	0 0	0 0	0 0

TABLE II. (Continued.)

Wyckoff position	1a(0 0 z)				1b(1/2 1/2 z)4d(x x z)				4e(x 0 z) → x ~ 1/3 z ~ -1/4; x ~ 1/3 z ~ 1/4				
	z ~ -1/4; z ~ 1/4		x ~ 1/6 z ~ -1/4; x ~ 1/6 z ~ 1/4		x ~ 1/3 z ~ -1/4; x ~ 1/3 z ~ 1/4		x ~ 1/3 z ~ -1/4; x ~ 1/3 z ~ 1/4		4f(x 1/2 z) → x ~ 1/6 z ~ -1/4; x ~ 1/6 z ~ 1/4				
i^a	1	1	2	3	4	1	2	3	4	1	2	3	4
	0 0 z					x 0 z	-x 0 z	0 x z	0 -x z	x 1/2 z	-x -1/2 z	-1/2 x z	1/2 -x z
	1/2 1/2 z	x x z	-x -x z	-x x z	x -x z								
n						3							
S_x^k		0 0	0 0	0 0	0 0	0 0	0 0	0 0	0 0	0 0	0 0	0 0	0 0
S_y^k		0 0	0 0	0 0	0 0	0 0	0 0	0 0	0 0	0 0	0 0	0 0	0 0
S_z^k		1 $\bar{1}$	$\bar{1}$ 1	1 1	$\bar{1}$ $\bar{1}$	0 1	0 $\bar{1}$	$\bar{1}$ 0	1 0				

^a i numerates cobalt ions in the 1a/1b, 4d, and 4e/4f positions; the coordinates of the symmetry linked ions are presented too.

^b n numerates sets of basis functions for irreps entering several times the magnetic representation.

^c j numerates sets of basis functions for many-dimensional irreps.

posed in Ref. 12 for the spin-state-ordered phase [Fig. 3(d)], revealed their identity (at the same values of the magnetic moments on paramagnetic cobalt ions). This means that a refinement of the neutron diffraction spectra in the model shown in Fig. 2(b) will give also good agreement with the experimental data. This can be considered as an experimental confirmation of the magnetic structures proposed here.

From Fig. 2(b) it clearly follows that the metamagnetic transition from the antiferromagnetic state into the state with spontaneous magnetization can be most easily induced by a magnetic field applied along the a direction, which is really observed in the experiment.^{13,14} Further, it is necessary to note that in spite of the strong difference in the models, the arguments, given by Taskin *et al.*¹³ to explain the thermal-induced transition from the antiferromagnetic to the ferromagnetic state and the strong correlation between electrical and magnetic properties, are entirely valid in our case. The magnetic structure shown in Fig. 2(b) suggests positive exchange interactions between fivefold-coordinated cobalt ions divided by [TbO_{0.5}] layers. Apparently, these interactions are caused by a complex indirect superexchange involving more than one oxygen ion and they are much weaker than the usual 180° exchange interactions. At increasing temperature short-time excitations of cobalt ions from the diamagnetic (Co³⁺ low-spin electronic configuration) state to the paramagnetic (Co³⁺ high-spin electronic configuration or Co²⁺/Co⁴⁺) one occur more often. The excited ions antiferromagnetically interact with the nearest neighbors, giving rise to magnetic frustrations. The transition to the state with spontaneous magnetization allows one to avoid the frustrations, because in this state all the nearest neighbors of the excited ion have an antiparallel spin (antiparallel to the spin of the excited ion). Moreover, the activation energy for the carrier generation, via the excited paramagnetic states, should be lower in the phase without frustrations—i.e., with the spin configuration shown in Fig. 2(a). This is the reason why the phase transition to the state with spontaneous magnetization is accompanied by a jump of the resistivity.

Let us show now that the obtained models can be easily extrapolated to LBaCo₂O_{5.44} compounds with the 332 type of crystal structure. Since in this crystal structure each cobalt ion with octahedral coordination has also four sixfold-coordinated nearest neighbors [Fig. 1(b)], it is quite logical to assume that a gain of elastic energy is enough for the ordering of cobalt ions in different spin states to be realized too. To avoid a cooperative character of the distortions in the (001) planes, containing cobalt ions in different spin states (due to a difference in the ionic radii of cobalt ions in the high- and low-spin states), the ordering should be like that shown in Fig. 4. In this case, the crystal structure is described by the $P4mm$ space group with the $3\sqrt{2}a_p \times 3\sqrt{2}a_p \times 2a_p$ unit cell. The ferrimagnetic structure originating from the G -type antiferromagnetic one (Fig. 4) is also characterized by the propagation vector $k=0$ (obligatory condition for a nonzero spontaneous moment) and can provide all the features of the magnetic behavior described above for the compounds with the 122 type of crystal structure.

To confirm that the proposed magnetic structure is consistent with the symmetry, the content of the magnetic representations on the 1a, 1b, 4d, 4e, and 4f cobalt positions in the $P4mm$ space group has been found:

$$D_m^{k=0}(1a) = D_m^{k=0}(1b) = \Gamma_4 + \Gamma_5,$$

$$D_m^{k=0}(4d) = \Gamma_1 + 2\Gamma_2 + \Gamma_3 + 2\Gamma_4 + 3\Gamma_5,$$

$$D_m^{k=0}(4e) = D_m^{k=0}(4f) = \Gamma_1 + \Gamma_2 + 2\Gamma_3 + 2\Gamma_4 + 3\Gamma_5. \quad (3)$$

The corresponding basis functions are presented in Table II. From the result it follows that the magnetic structure, shown in Fig. 4, can be constructed using the basis functions of the single $\Gamma_4(n=1)$ irreducible representation of the $P4mm$ space group, which is consistent with the symmetry requirement. However, it should be noted that since cobalt ions occupy positions with different transformational properties in the

$P4mm$ space group, the requirement of a single irrep mediation for the entire magnetic structure is not rigid.

By analogy with $LBaCo_2O_{5.5}$, the low-temperature (below T_i) antiferromagnetic structure for $LBaCo_2O_{5.44}$ can be obtained by doubling the magnetic unit cell along the $[001]$ direction.

In conclusion, symmetry considerations and analysis of the previously reported magnetic, magnetotransport, and neutron diffraction data allowed us to conclude that the

$LBaCo_2O_{5.5/5.44}$ cobalt oxides demonstrate an exotic type of electronic ordering, involving a translational symmetry distribution of sixfold-coordinated cobalt ions in low- and high-spin states. The proposed magnetic structures are consistent with the symmetry constraints and resolve contradictions between the results of the magnetic measurements and neutron diffraction experiments as well as give a clear picture of the magnetic behavior of these compounds.

-
- ¹C. Martin, A. Maignan, D. Pelloquin, N. Nguyen, and B. Raveau, *Appl. Phys. Lett.* **71**, 1421 (1997).
- ²I. O. Troyanchuk, N. V. Kasper, D. D. Khalyavin, H. Szymczak, R. Szymczak, and M. Baran, *Phys. Rev. Lett.* **80**, 3380 (1998).
- ³I. O. Troyanchuk, N. V. Kasper, D. D. Khalyavin, H. Szymczak, R. Szymczak, and M. Baran, *Phys. Rev. B* **58**, 2418 (1998).
- ⁴A. Maignan, C. Martin, D. Pelloquin, N. Nguyen, and B. Raveau, *J. Solid State Chem.* **142**, 247 (1999).
- ⁵D. Akahoshi and Y. Ueda, *J. Solid State Chem.* **156**, 355 (2001).
- ⁶D. D. Khalyavin, A. M. Balagurov, A. I. Beskrovnyi, I. O. Troyanchuk, A. P. Sazonov, E. V. Tsipis, and V. V. Kharton, *J. Solid State Chem.* **177**, 2068 (2004).
- ⁷E. Suard, F. Fauth, V. Caignaert, I. Mirebeau, and G. Baldinozzi, *Phys. Rev. B* **61**, R11871 (2000).
- ⁸F. Fauth, E. Suard, V. Caignaert, B. Domenges, I. Mirebeau, and L. Keller, *Eur. Phys. J. B* **21**, 163 (2001).
- ⁹N. V. Kasper, I. O. Troyanchuk, D. D. Khalyavin, N. Hamad, L. Haupt, P. Frobel, K. Barner, E. Gmelin, Q. Huang, and J. W. Lynn, *Phys. Status Solidi B* **215**, 697 (1999).
- ¹⁰D. Akahoshi and Y. Ueda, *J. Phys. Soc. Jpn.* **68**, 736 (1999).
- ¹¹H. Wu, *Phys. Rev. B* **64**, 092413 (2001).
- ¹²F. Fauth, E. Suard, V. Caignaert, and I. Mirebeau, *Phys. Rev. B* **66**, 184421 (2002).
- ¹³A. A. Taskin, A. N. Lavrov, and Y. Ando, *Phys. Rev. Lett.* **90**, 227201 (2003).
- ¹⁴D. D. Khalyavin, S. N. Barilo, S. V. Shiryayev, G. L. Bychkov, I. O. Troyanchuk, A. Furrer, P. Allenspach, H. Szymczak, and R. Szymczak, *Phys. Rev. B* **67**, 214421 (2003).
- ¹⁵H. D. Zhou and J. B. Goodenough, *J. Solid State Chem.* **177**, 3339 (2004).
- ¹⁶M. Itoh, Y. Nawata, T. Kiyama, D. Akahoshi, N. Fujiwara, and Y. Ueda, *Physica B* **329**, 751 (2003).
- ¹⁷H. Kubo, K. Zenmyo, M. Itoh, N. Nakayama, Y. Mizota, and Y. Ueda, *J. Magn. Magn. Mater.* **272**, 581 (2004).
- ¹⁸Yu. P. Chernenkov, V. P. Plakhty, V. I. Fedorov, S. N. Barilo, S. V. Shiryayev, and G. L. Bychkov, *Phys. Rev. B* **71**, 184105 (2005).
- ¹⁹D. L. Khomskii and U. Low, *Phys. Rev. B* **69**, 184401 (2004).
- ²⁰J. F. Mitchell, J. Burley, and S. Sort, *J. Appl. Phys.* **93**, 7364 (2003).
- ²¹C. S. Knee, D. J. Price, M. R. Lees, and M. T. Weller, *Phys. Rev. B* **68**, 174407 (2003).
- ²²Z. Hu, H. Wu, M. W. Haverkort, H. H. Hsieh, H. J. Lin, T. Lorenz, J. Baier, A. Reichl, I. Bonn, C. Felser, A. Tanaka, C. T. Chen, and L. H. Tjeng, *Phys. Rev. Lett.* **92**, 207402 (2004).
- ²³H. Wu, *Phys. Rev. B* **62**, R11953 (2000).
- ²⁴S. C. Miller and W. F. Love, *Tables of Irreducible Representations of Space Groups and Co-Representations of Magnetic Space Groups*, 4th ed. (Prentice Hall, Englewood Cliffs, 1967).
- ²⁵M. Soda, Y. Yasui, T. Fujita, M. Sato, and K. Kakurai, *J. Phys. Soc. Jpn.* **72**, 1729 (2003).
- ²⁶C. Frontera, J. L. Garcia-Munoz, A. Llobet, and M. A. G. Aranda, *Phys. Rev. B* **65**, 180405(R) (2002).
- ²⁷A. Maignan, V. Caignaert, B. Raveau, D. Khomskii, and G. Sawatzky, *Phys. Rev. Lett.* **93**, 026401 (2004).
- ²⁸W. R. Flavell, A. G. Thomas, D. Tsoutsou, A. K. Mallick, M. North, E. A. Seddon, C. Cacho, A. E. R. Malins, S. Patel, R. L. Stockbauer, R. L. Kurtz, P. T. Sprunger, S. N. Barilo, S. V. Shiryayev, and G. L. Bychkov, *Phys. Rev. B* **70**, 224427 (2004).
- ²⁹J. Rodriguez-Carvajal, *Physica B* **192**, 55 (1993).